Biocompatibility of Fe_3O_4 nanoparticles evaluated by *in vitro* cytotoxicity assays using normal, glia and breast cancer cells

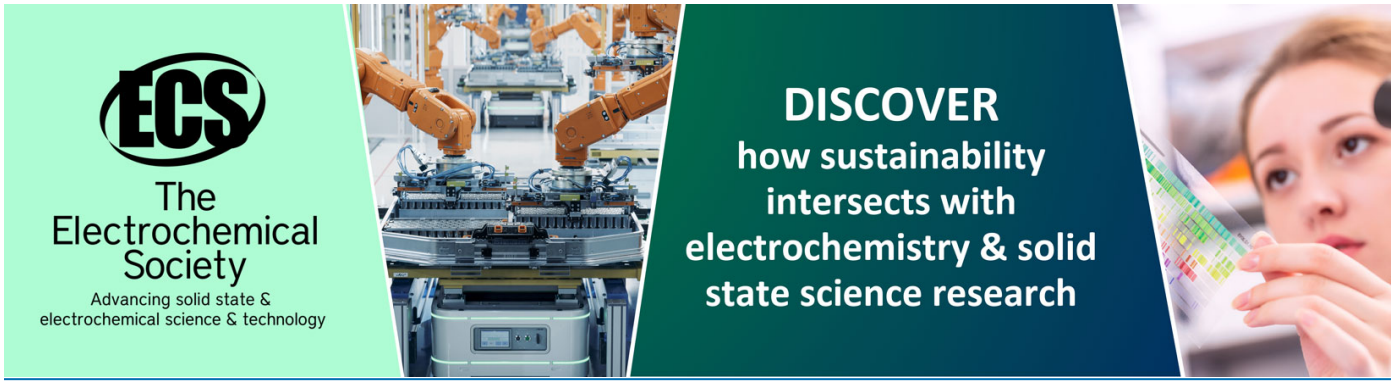

Nanotechnology **21** (2010) 075102 (9pp) doi:10.1088/0957-4484/21/7/075102

Biocompatibility of Fe_3O_4 nanoparticles evaluated by *in vitro* cytotoxicity assays using normal, glia and breast cancer cells

B Ankamwar[1], T C Lai[2], J H Huang[1], R S Liu[1,4], M Hsiao[2], C H Chen[2] and Y K Hwu[3]

[1] Department of Chemistry, National Taiwan University, Taipei 106, Taiwan
[2] Genomics Research Center, Academia Sinica, Taipei 115, Taiwan
[3] Institute of Physics, Academia Sinica, Taipei 115, Taiwan

E-mail: rsliu@ntu.edu.tw

Received 8 September 2009, in final form 25 December 2009
Published 21 January 2010
Online at stacks.iop.org/Nano/21/075102

Abstract

In order to reveal the biocompatibility of Fe_3O_4 nanoparticles and bipolar surfactant tetramethylammonium 11-aminoundecanoate cytotoxicity tests were performed as a function of concentration from low (0.1 μg ml^{-1}) to higher concentration (100 μg ml^{-1}) using various human glia, human breast cancer and normal cell lines. Cytotoxicity tests for human glia (D54MG, G9T, SF126, U87, U251, U373), human breast cancer (MB157, SKBR3, T47D) and normal (H184B5F5/M10, WI-38, SVGp12) cell lines exhibited almost nontoxicity and reveal biocompatibility of Fe_3O_4 nanoparticles in the concentration range of 0.1–10 μg ml^{-1}, while accountable cytotoxicity can be seen at 100 μg ml^{-1}. The results of our studies suggest that Fe_3O_4 nanoparticles coated with bipolar surfactant tetramethylammonium 11-aminoundecanoate are biocompatible and promising for bio-applications such as drug delivery, magnetic resonance imaging and magnetic hyperthermia.

(Some figures in this article are in colour only in the electronic version)

1. Introduction

Testing for cytotoxicity is indispensable towards ensuring the biocompatibility of a medical device for biomedical applications. It is simply a first step. On the other hand, a positive cytotoxicity test result can be taken as an early warning sign that a material contains one or more extractable substances that could be of clinical importance. In such cases, further investigation is required to determine the utility of the material.

The targeted delivery of magnetic nanoparticles [1, 2], loaded with drugs [3] or genes [4], has been of increasing interest in cancer therapy. The exciting applications of these particles could be in magnetic hyperthermia (heating via AC magnetic fields) [5, 6] of tumors. The cells can be placed, tracked and recovered using a magnetic resonance imaging (MRI) technique if a high concentration of magnetic nanoparticles is used [7–9]. However, the preparation of stable Fe_3O_4 nanoparticles with high concentration in biocompatible solutions is difficult. In spite of very interesting and potential biomedical applications, the concentration level at which Fe_3O_4 nanoparticles become toxic has remained so far unclear. It is generally believed that Fe_3O_4 [10, 11] nanoparticles are biocompatible in biological systems. However, this important issue remains controversial: various reports revealed close links between toxicity and nanoparticle size [12], concentration [7], surface properties [13–15] and surface coating by hydroxyapatite [16], protein [17] and chitosan molecules [18].

In the present work, the biocompatibility of Fe_3O_4 nanoparticles was evaluated by *in vitro* cytotoxicity assay for their potential *in vivo* biomedical applications such as targeted drug delivery [19, 20], cancer cell diagnostics [21–24] and therapeutics [16]. Large near-infrared (NIR) absorption of gold nanotriangles could be used in the hyperthermia of tumors [25–27]. Many groups have investigated the acute cytotoxicity of magnetic nanoparticles [28–30], antibiotic-conjugated polyacrylate nanoparticles [31] and their qualitative effects upon cellular morphology. However, little work

[4] Author to whom any correspondence should be addressed.

has been focused on quantifying the effects of magnetic nanoparticles upon cell behavior. Cytotoxicity studies of poly(lactide-co-glycolide) nanoparticles against HCT116 cells [32] and various ferrite nanoparticles against human cervical HeLa cancer cells [33] were carried out.

To the best of our knowledge, the internalization of Fe_3O_4 nanoparticles and possible cytotoxicity with different kinds of cell lines such as human glia D54MG, G9T, SF126, U87, U251 and U373, human breast cancer MB157, SKBR3 and T47D and normal H184B5F5/M10, WI-38 and SVGp12 cell lines were not sufficiently analyzed. *In vitro* cytotoxicity assays showed that the Fe_3O_4 nanoparticles are nontoxic at lower concentrations from 0.1 to 10 μg ml^{-1}, while accountable cytotoxicity can be seen at higher concentrations of 100 μg ml^{-1}. Thus our study on the biocompatibility of Fe_3O_4 nanoparticles evaluated by *in vitro* cytotoxicity assays using normal, glia and breast cancer cells may serve as an improved way of targeting drug delivery and hyperthermia of tumors.

2. Methods and materials

2.1. Nanoparticle synthesis

Fe_3O_4 nanoparticles were synthesized using a slightly modified protocol [34, 35]. Briefly, 0.71 g ferric acetylacetonate (Sigma-Aldrich) was mixed with 20 ml of phenyl ether (Sigma-Aldrich), 2 ml of oleic acid (Sigma-Aldrich), 2 ml of oleylamine (Acros Chemicals) and 2.303 g of 1,2-tetradecanediol (Sigma-Aldrich) under argon atmosphere with vigorous stirring. The reaction mixture was heated to 210 °C and refluxed for 1.5 h. Ethanol was added to the solution after cooling to room temperature. A dark-black precipitate was separated by centrifugation at 10 000 rpm for 15 min. After washing with ethanol the nanoparticles were collected by centrifugation at 10 000 rpm and re-dispersed in hexane in the presence of 75 mM each of oleic acid and oleylamine.

2.2. Phase transfer of Fe_3O_4 nanoparticles from organic to aqueous media

Hydrophobic Fe_3O_4 particles were transferred from hexane to aqueous solution using a bipolar surfactant, tetramethylammonium 11-aminoundecanoate [34, 36]. Briefly a methanolic suspension of 11-aminoundecanoic acid (Sigma-Aldrich) (4.04 g in ∼7 ml methanol) was titrated with methanolic tetramethylammonium hydroxide (15 ml) (Sigma-Aldrich), followed by evaporation of the solvent under reduced pressure, and recrystallization from tetrahydrofuran (∼50 ml) (Sigma-Aldrich). For the phase transfer, 0.035 g surfactant was suspended in ∼2.5 ml of dichloromethane (Sigma-Aldrich) and 0.05 ml of the hydrophobic Fe_3O_4 colloid was added. The mixture was placed on a shaker for ∼1.5 h leading to a complete phase transfer. The phase-transferred Fe_3O_4 nanoparticles were separated using a centrifugation method at 14 000 rpm for 15 min. The nanoparticles were re-dispersed in millipore water. The particles were washed from excess surfactant by removing the supernatant after centrifugation and then re-dispersing in millipore water.

2.3. Surface-charge determination of the Fe_3O_4 nanoparticles

Surface-charge determination of the Fe_3O_4 nanoparticles was performed at pH 7.4 using tris-borate-EDTA (TBE) buffer, 1% agarose gel and an applied voltage of 100 V for 20 min.

2.4. Zeta potential determination of the suspensions of the nanoparticles

The zeta potential determination of the suspensions of Fe_3O_4 nanoparticles was performed in PBS solution under 532 nm laser by a Zetasizer 3000HS.

2.5. XRD analysis of the Fe_3O_4 nanoparticles

The x-ray diffraction patterns of the Fe_3O_4 nanoparticles were recorded with the use of a BL01C2 ($\lambda = 0.774\,903$ Å) light source at the National Synchrotron Radiation Research Center (NSRRC), Hsinchu, Taiwan.

2.6. Fourier transform infrared (FTIR) analysis

In order to reveal some interactions of nanoparticles with the organic phase, samples were mixed with IR grade KBr and subjected to FTIR analysis on a Perkin-Elmer FTIR spectrophotometer in the diffuse reflectance mode at a resolution of 4 cm^{-1}.

2.7. Characterization of nanoparticles

The morphology of Fe_3O_4 nanoparticles was characterized by transmission electron microscopy (TEM) (JEOL-1200 EX operating at an accelerating voltage of 80 kV). The nanoparticle samples dispersed in hexane solution and in aqueous media were cast onto a carbon-coated copper grid sample holder, followed by evaporation at room temperature.

Ultraviolet–visible (UV–vis) spectra were obtained with a Shimadzu UV-1700 UV–visible spectrophotometer. The spectra were recorded over the range 200–1100 nm. Particle size was determined from TEM images using Matrox Inspector 2.2 software.

2.8. Cell cultures

This study was carried out using nine cancer cell lines and three normal cell lines. There were two cancer cell types, human glia and human breast cancer. Human glia cell lines contained D54MG, G9T, SF126, U87, U251 and U373. Human breast cancer cell lines contained MB157, SKBR3 and T47D. SVGp12 was a SV40 transformed human embryonic astroglia cell as a normal control of glioma. H184B5F5/M10 was an irradiation transformed human mammary epithelial cell as a control of breast cancer. WI-38 was a human normal lung fibroblast. Among these cell lines, D54MG, G9T, SF126, MB157, U87, U251 and U373 were cultured in Dulbecco's modified Eagle's medium (DMEM). SKBR3 and T47D were cultured in RPMI medium 1640. SVGp12 and WI-38 were cultured in minimum essential medium (MEM) with 0.1 mM non-essential amino acids and 1.0 mM sodium pyruvate. H184B5F5/M10 was cultured in alpha-minimum essential medium (alpha-MEM). All media also contained

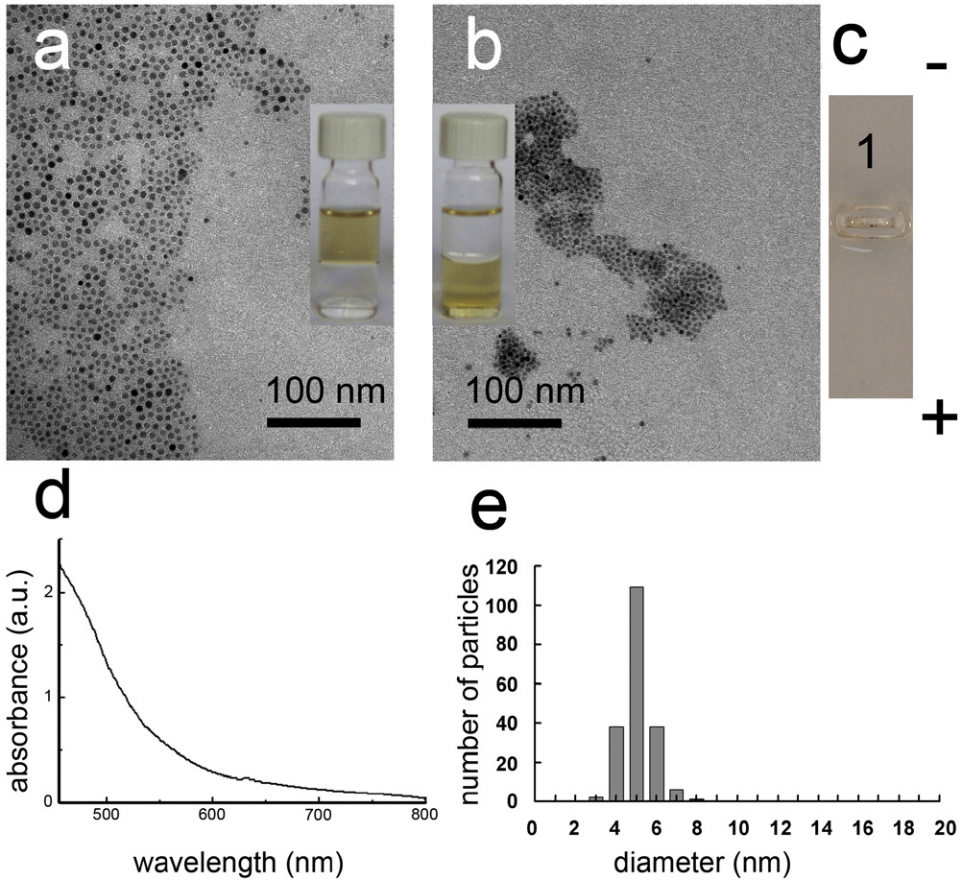

Figure 1. TEM micrographs of Fe_3O_4 nanoparticles in hexane represented by (a) and in water (b); surface-charge determination by gel electrophoresis (pH 7.4, 100 V, 1% agarose gel and TBE buffer) for Fe_3O_4 in aqueous media (c). UV–vis spectra of Fe_3O_4 corresponding to sample in aqueous media (d). Size distribution panel of Fe_3O_4 nanoparticles in aqueous media.

2 mM L-glutamine, 100 units ml^{-1} penicillin, 100 $\mu g\ ml^{-1}$ streptomycin and 10% fetal bovine serum. These cells were maintained at 37 °C, under 5% CO_2 for 24 h. At this point cells were incubated in complete medium supplemented with 0.1–100 $\mu g\ ml^{-1}$ of Fe_3O_4 nanoparticles for a further 72 h. All control cells were cultured in the absence of nanoparticles.

2.9. Cell viability assay

To determine the cell viability/toxicity, the cells were plated at a density of 2×10^3 cells/well in a 96-well plate at 37 °C, under 5% CO_2. The nanoparticles in varying concentrations from 0.1 to 100 $\mu g\ ml^{-1}$ were prepared in phosphate buffered saline (PBS) and added at the same time when plating cells. To get the net value of absorbance from the cells, the absorbance of each well was measured at 490 nm, before addition of (3-(4,5-dimethylthiazol-2-yl)-5-(3-carboxymethoxyphenyl)-2-(4-sulfophenyl)-2H-tetrazolium, inner salt) MTS as a background value obtained due to nanoparticles. MTS contains the tetrazolium compound (3-(4,5-dimethylthiazol-2-yl)-5-(3-carboxymethoxyphenyl)-2-(4-sulfophenyl)-2H-tetrazolium, inner salt) and an electron coupling reagent (phenazine ethosulfate; PES) to form a stable solution. After 72 h, 20 μl of MTS (Promega) was added to each well. After 1 h of incubation at 37 °C, the absorbance of each well was read on a microplate reader (Tekon, SpectraMax M2) at 490 nm. The spectrophotometer was calibrated to zero absorbance, using culture medium without cells. The quantity of formazan product as measured by the absorbance at 490 nm is directly proportional to the number of living cells in the culture. The relative cell viability (%) related to control wells containing cell culture medium without nanoparticles was calculated by $[A]_{test}/[A]_{control} \times 100$, where $[A]_{test}$ is the absorbance of the test sample and $[A]_{control}$ is the absorbance of the control sample. The images of cancer cell lines were acquired by 400× magnification by an Olympus IX71 microscope.

3. Results

3.1. Characterization of nanoparticles

Fe_3O_4 nanoparticles were synthesized according to a well-established procedure [34, 35] with slight modification, followed by phase transfer from the organic to aqueous media using a bipolar surfactant, tetramethylammonium 11-aminoundecanoate [34, 36]. The Fe_3O_4 solution was centrifuged at 14 000 rpm for 15 min followed by washing twice with millipore water and recollected by centrifugation.

Figures 1(a) and (b) show a representative TEM images of the Fe_3O_4 nanoparticles collected from the above separation

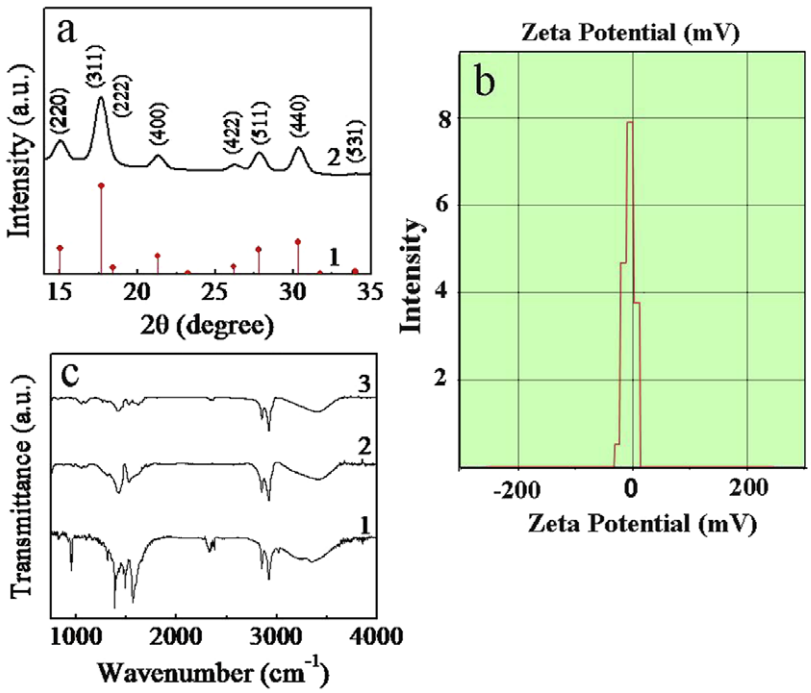

Figure 2. The x-ray diffraction patterns of the standard (a1) and as-prepared (a2) Fe_3O_4 nanoparticles; (b) the zeta potential of the suspensions of Fe_3O_4 nanoparticles; (c1) FTIR spectra of the bipolar surfactant, Fe_3O_4 nanoparticles in organic (c2) and aqueous (c3) media.

processes in hexane and water, respectively. To examine the surface charge of the precipitates of nanoparticles by agarose gel electrophoresis (1%, an applied voltage of 100 V cm^{-1}, TBE buffer) of Fe_3O_4 (shown in figure 1(c)) was performed at pH 7.4, since the pH of blood is 7.4, which would be one of the important factors needed to be considered to extend this work to an *in vivo* study. Here, the result of electrophoresis did not reveal migration of Fe_3O_4 nanoparticles to either positive or negative electrodes, owing to the zero surface potential as a pH 7.4 medium is used.

UV–vis spectra of Fe_3O_4 nanoparticles in water did not show any characteristic surface plasmons (SP) in the visible region of the electromagnetic spectrum (figure 1(d)). The diameter statistics plot of Fe_3O_4 nanoparticles reveals monodisperse Fe_3O_4 nanoparticles with an average diameter ∼5 nm (figure 1(e)).

Figures 2(a1) and (a2) show the x-ray diffraction patterns of the standard Fe_3O_4 and as-prepared Fe_3O_4 nanoparticles, respectively. The 2θ values of the standard Fe_3O_4 nanoparticles 14.973°, 17.583°, 18.378°, 21.256°, 26.0998°, 27.7185°, 30.2250° and 33.90° correspond to the Bragg reflections (220), (311), (222), (400), (422), (511), (440) and (531), respectively, whereas the 2θ values of as-prepared Fe_3O_4 nanoparticles 15.044°, 17.652°, 21.32°, 26.33°, 27.831°, 30.04° and 34.04° correspond to the Bragg reflections (220), (311), (400), (422), (511), (440) and (531), respectively. In consideration of the wavelength of the light source BL01C2 ($\lambda = 0.774\,903$ Å) our 2θ values are almost a match with JCPDF file no. 79-0419 for Fe_3O_4 (magnetite).

The average of three runs of zeta potential (−0.9, +2.0 and −1.5 mV) of the suspensions of Fe_3O_4 nanoparticles was −0.1 mV (figure 2(b)). The value is almost very close to zero. We agree that a Z potential near zero is not convenient at the isoelectric point. However, these are macroscopic average measurements and hence do not reflect the localized charges of these nanoparticles. Hence our experimental results on electrophoresis cannot be correlated with their charges in zeta potential value.

FTIR spectra of bipolar surfactant (figure 2(c1)) and Fe_3O_4 nanoparticles in organic (figure 2(c2)) and aqueous (figure 2(c3)) media give a clear indication that the nanoparticles of Fe_3O_4 are coated with a surfactant. We have modified the Fe_3O_4 nanoparticle surface by replacing the oleate species using the tetramethylammonium 11-aminoundecanoate ligand to promote hydrophilicity [34].

The carboxylate group of the ligand binds to the surface iron and exposes the hydrophilic amino group to aqueous media. This can be revealed by the shifting of a strong asymmetrical stretching carboxylate band of the bipolar surfactant from 1561 to 1527 cm^{-1}, and C–O stretching and O–H deformation from 1311 to 1261 cm^{-1} [37, 38].

3.2. Cytotoxicity of bipolar surfactant towards cancer cell lines

One could suspect a surfactant coating of Fe_3O_4 nanoparticles may adversely impact the toxicity examination. To clarify this issue, the bipolar surfactant, tetramethylammonium 11-aminoundecanoate, was analyzed to examine the possible cytotoxicity. Figure 3(a) shows representative bright-field microscopy images with 400× magnification at maximum exposure dosage (100 $\mu g\ ml^{-1}$) after incubating with normal lung fibroblast WI-38 cell line, normal glia cell line (SVGp12), glia cancer cell lines (D54MG, G9T/VGH, SF126, U87, U251

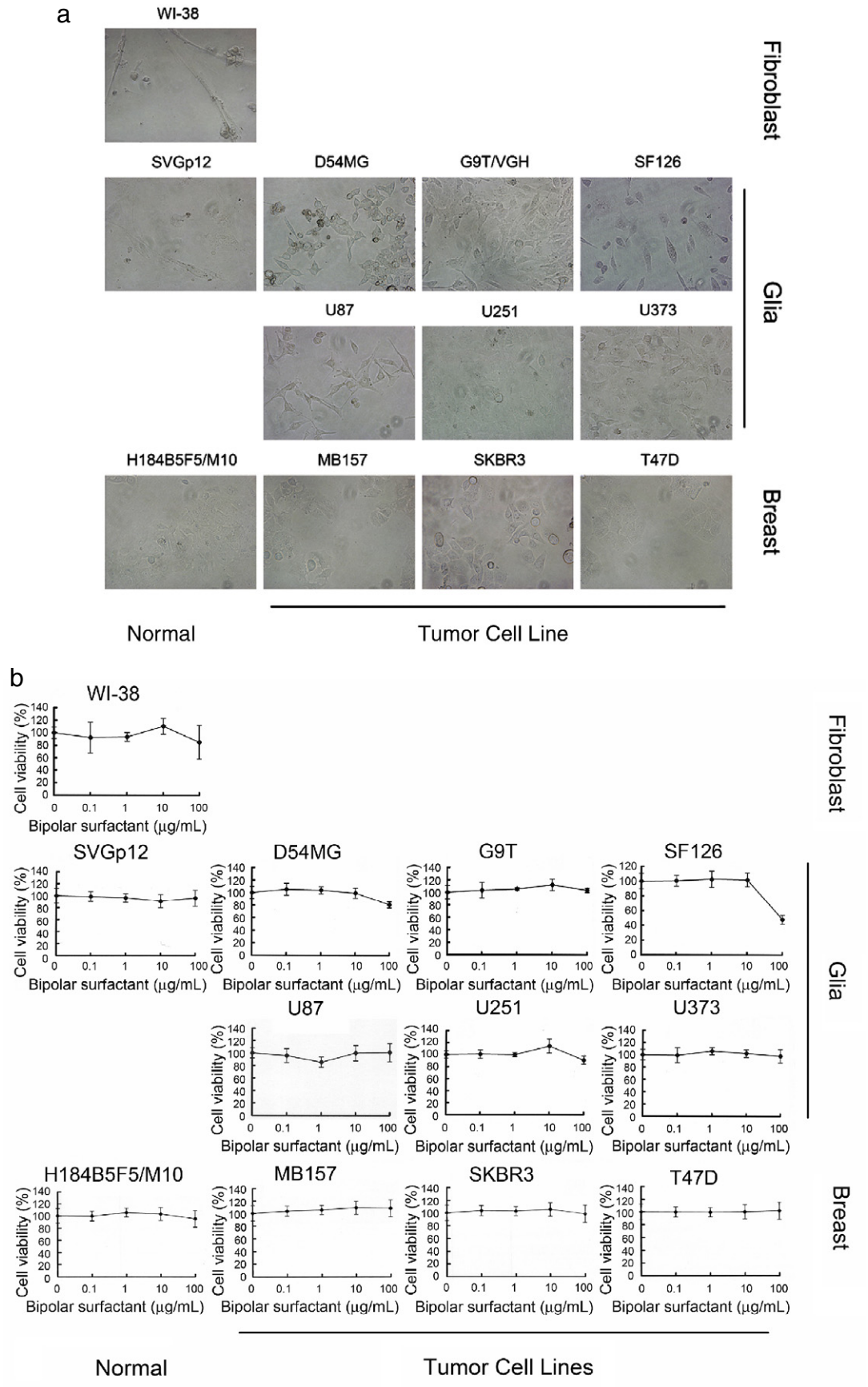

Figure 3. (a) Bright-field microscopy of various cell images with 400× magnification after incubating with surfactant at maximum exposure dosage (100 μg ml^{-1}) for 72 h. (b) Cell viability curves for each cell line incubated with surfactant dosage in the range from 0.1 to 100 μg ml^{-1} for 72 h.

Table 1. Percentage cell viability at various exposure dosages (0.1–100 μg ml^{-1}) of bipolar surfactant.

Cell line	Surfactant 0.1 (μg ml^{-1})	Surfactant 1 (μg ml^{-1})	Surfactant 10 (μg ml^{-1})	Surfactant 100 (μg ml^{-1})
WI-38	92.4 ± 24.5	93.6 ± 7.1	110.4 ± 12.5	84.9 ± 26.9
SVGp12	98.5 ± 8.1	96.4 ± 7.2	90.8 ± 10.7	95.9 ± 13.6
D54MG	105.3 ± 9.5	103.6 ± 5.7	99.1 ± 8.1	80.5 ± 5.1
G9T/VGH	103.2 ± 12.5	105.3 ± 2.1	112.0 ± 9.1	103.3 ± 3.6
SF126	100.6 ± 7.1	102.7 ± 10.9	101.8 ± 9.2	47.8 ± 5.8
U87	95.7 ± 11.0	85.1 ± 8.1	99.6 ± 12.4	100.5 ± 14.5
U251	100.8 ± 7.0	99.9 ± 3.5	114.1 ± 11.7	90.8 ± 6.9
U373	99.2 ± 12.1	105.9 ± 5.9	102.1 ± 6.2	97.7 ± 11.1
H184B5F5/M10	99.4 ± 21.0	105.1 ± 13.3	102.9 ± 13.6	95.1 ± 11.0
MB157	103.5 ± 4.6	105.4 ± 5.0	108.9 ± 5.2	108.2 ± 7.3
SKBR3	103.4 ± 22.0	102.7 ± 20.2	105.3 ± 20.2	98.4 ± 22.9
T47D	99.6 ± 6.0	99.2 ± 6.9	99.8 ± 11.3	101.5 ± 8.1

Table 2. Percentage cell viability at various exposure dosages (0.1–100 μg ml^{-1}) of Fe_3O_4 nanoparticles.

Cell line	Fe_3O_4 0.1 (μg ml^{-1})	Fe_3O_4 1 (μg ml^{-1})	Fe_3O_4 10 (μg ml^{-1})	Fe_3O_4 100 (μg ml^{-1})
WI-38	93.3 ± 6.8	98.8 ± 22.5	99.3 ± 12.3	114.7 ± 17.2
SVGp12	94.1 ± 4.7	105.0 ± 8.8	97.7 ± 4.4	78.8 ± 8.3
D54MG	112.2 ± 14.1	112.7 ± 15.7	95.8 ± 6.4	69.8 ± 12.1
G9T/VGH	101.7 ± 1.7	109. ± 9.0	96.5 ± 9.1	76.5 ± 10.9
SF126	94.18 ± 3.8	94.0 ± 5.4	99.9 ± 2.1	93.6 ± 6.8
U87	100.7 ± 7.3	100.3 ± 7.9	99.0 ± 7.5	91.4 ± 10.3
U251	107.2 ± 7.1	107.5 ± 6.4	108.6 ± 6.4	75.4 ± 7.2
U373	104.4 ± 9.9	100.5 ± 12.0	93.5 ± 9.7	91.6 ± 8.2
H184B5F5/M10	96.6 ± 1.8	99.5 ± 5.0	100.3 ± 7.6	80.4 ± 10.0
MB157	102.9 ± 8.3	99.7 ± 4.0	102.4 ± 9.2	90.5 ± 6.2
SKBR3	109.7 ± 11.0	121.3 ± 12.3	137.2 ± 8.1	105.5 ± 12.4
T47D	95.6 ± 4.4	93.4 ± 2.3	95.2 ± 6.2	81.8 ± 7.6

and U373), normal breast epithelial cell line (H184B5F5/M10) and breast cancer cell lines (MB157, SKBR3 and T47D) for 72 h. The MTS data as shown in figure 3(b) indicates that the bipolar surfactant is almost nontoxic in the range of 0.1–10 μg ml^{-1}. However, the WI-38, D54MG and SF-126 cell lines show cytotoxicity at 100 μg ml^{-1}. The surfactant was found to be more toxic in the case of SF126 at 100 μg ml^{-1}.

3.3. Cytotoxicity of Fe_3O_4 nanoparticles towards cancer cell lines

Figure 4(a) shows representative bright-field microscopy images of normal fibroblast WI-38 cell line, normal glia cell line (SVGp12), glia cancer cell lines (D54MG, G9T/VGH, SF126, U87, U251 and U373), normal breast epithelial cell line (H184B5F5/M10) and breast cancer cell lines (MB157, SKBR3 and T47D) after incubating with Fe_3O_4 nanoparticles at maximum exposure dosage (100 μg ml^{-1}) for 72 h.

Figure 4(b) shows cell viability curves of Fe_3O_4 nanoparticles at maximum exposure dosage (100 μg ml^{-1}) after incubating with cells for 72 h. Fe_3O_4 nanoparticles are nontoxic for all cell lines in the range of 0.1–10 μg ml^{-1}. However, cell viability was found to be reduced at 100 μg ml^{-1} of Fe_3O_4 nanoparticles.

In SKBR3 and T47D cell lines, cell injury is clearly visible. However, in the rest of the cell lines, WI-38, D54MG,G9T/VGH, SF126, U87, U251, U373, H184B5F5/M10 and MB157, Fe_3O_4 nanoparticles entered into the cell membrane and nucleus. This reveals that there are attractive forces between the cell membrane and nanoparticles.

In table 1, the data of percentage cell viability at different bipolar surfactant concentrations reveals that more or less all cell lines are ∼100% viable below a surfactant concentration of 10 μg ml^{-1}. However, at a surfactant concentration up to 100 μg ml^{-1}, slightly reduced cell viability was observed in the case of normal fibroblast WI-38 and cancer cell lines D54MG and U251, except SF126 where it was found to be greatly reduced to 50%. Table 2, the percentage cell viability at different Fe_3O_4 concentrations, reveals that more or less all cell lines are ∼100% viable at and below Fe_3O_4 concentration of 10 μg ml^{-1}. However, at Fe_3O_4 concentration of 100 μg ml^{-1}, 10–25% cell viability was found to be reduced, except in the case of SKBR3 and WI-38 it was slightly increased.

4. Discussion

The use of Fe_3O_4 nanoparticles in cancer cell biology is well documented with various applications, e.g. targeted drug delivery [19, 20], cancer cell diagnostics [21–24] and therapeutics [16]. The latest study on particle stability in physiological conditions as well as biocompatibility has important issues for these applications. To provide an insight into the origin of toxicity towards cancer cells, Fe_3O_4 nanoparticles are fabricated using a bipolar surfactant. In this

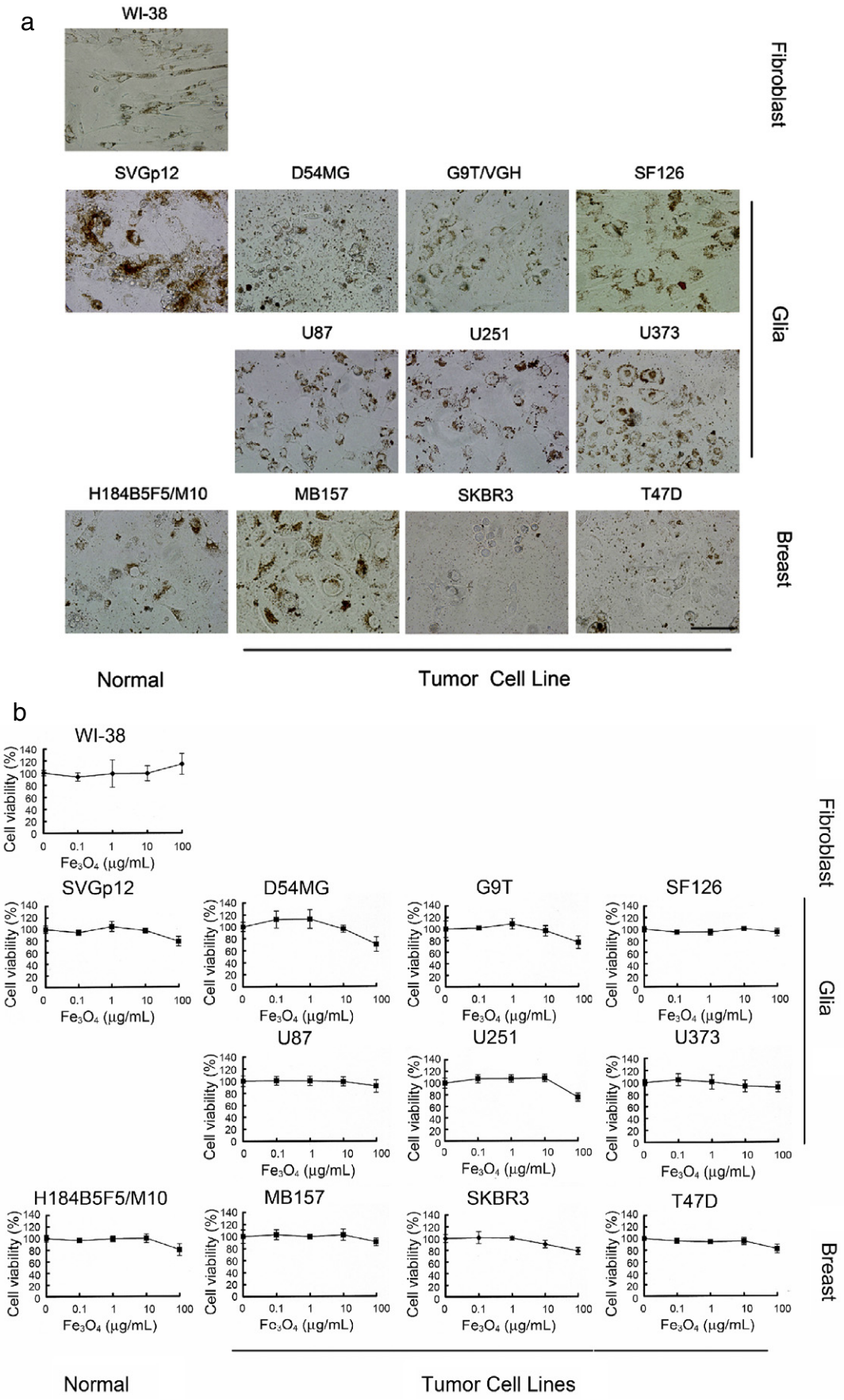

Figure 4. (a) Bright-field microscopy of various cell images with 400× magnification after incubating with Fe_3O_4 nanoparticles at maximum exposure dosage (100 μg ml^{-1}) cells for 72 h. (b) Cell viability curves for each cell line incubated with Fe_3O_4 nanoparticle dosage in the range from 0.1 to 100 μg ml^{-1} after incubating with cells for 72 h.

study, Fe_3O_4 nanoparticles were synthesized in organic media and phase-transferred to aqueous media, since hydrophilic nanoparticles have the additional advantage of prolonged circulation in the blood, which would facilitate the targeting of nanoparticles to the tumor cells [39].

The Fe_3O_4 nanoparticles preferentially associate with cancer cells (figure 4(a)). This may be due to interaction between surfactant and proteins on cancer cells through a $–NH_2$ functional group. Because of the large surface area to volume ratio, the magnetic nanoparticles tend to agglomerate and adsorb plasma proteins [11]. The dark brown color in the cell image appears on the surface of cells owing to the agglomeration of Fe_3O_4 nanoparticles, which show the dipolar surfactant can supply the nonspecific interaction for Fe_3O_4 nanoparticles to incorporate with the surface of cells. In glia cell lines (D54MG,G9T/VGH, SF126, U87, U251 and U373) and breast cell lines (MB157, SKBR3 and T47D), cell bubbles indicate cell death. Magnetite nanoparticles entered into the cell membrane and the nucleus of glia cells U373 and breast cells MB157 and formed necklace-like eccentric circles. This may be an indication of endocytosis. Figure 4(b) gives cell viability MTS results of Fe_3O_4 nanoparticles. Cell viability of all cell lines are almost unaffected up to 10 μg ml^{-1} Fe_3O_4 nanoparticles, but it was found to be reduced by an average ∼20% at 100 μg ml^{-1} of Fe_3O_4 nanoparticles except for WI-38, SF126, U87, U373, MB157 and SKBR3. To reveal the cause of this observation needs further study. Overall, it was revealed that the exposure of cells to high concentrations of Fe_3O_4 nanoparticles adversely affects cell function, phenotype and viability. Our findings also indicate and confirm previous reports that the presence of intracellular magnetic nanoparticles can result in significant changes in cell behavior and viability [9, 14, 28]. In this study observed cytotoxicity effects are difficult to diagnose but the following plausible explanations can support our observations as reported earlier by Pisanic *et al* [9]: first, coordination between surfactant and the nanostructures facilitates entry of both the nanostructures and surfactants into or interaction with the cells; secondly, the variance in effectiveness of the surfactants to shield the nanostructures from adverse interactions with cellular components and, thirdly, it may be a combination of both. The presence of Fe_3O_4 nanoparticles into or on the cells may obstruct transcriptional regulation and protein synthesis resulting in cell death [9]. Auffan *et al* [40], demonstrated the relationship between the redox state of iron-based nanoparticles and their cytotoxicity toward a Gram-negative bacterium, *Escherichia coli*. They [40] reported that the chemically stable nanoparticles (Fe_2O_3) have no apparent cytotoxicity, while nanoparticles containing ferrous and, particularly, zero-valent iron are cytotoxic. The cytotoxic effects appear to be associated principally with an oxidative stress as demonstrated using a mutant strain of *E. coli* completely devoid of superoxide dismutase activity. This stress can result from the generation of reactive oxygen species with the interplay of oxygen with reduced iron species (FeII and/or Fe) or from the disturbance of the electronic and/or ionic transport chains due to the strong affinity of the nanoparticles for the cell membrane. A similar mechanism may be operative in our study causing stress which could be the result of the generation of reactive oxygen species with the interplay of oxygen with reduced iron species (Fe^{3+}/Fe^{2+}) or from the disturbance of the electronic and/or ionic transport chains due to the strong affinity of the nanoparticles for the cell membrane.

5. Conclusions

In summary, Fe_3O_4 nanoparticles were synthesized and phase-transferred from organic to aqueous media. Fe_3O_4 nanoparticles exhibited almost nontoxicity in the range of 0.1–10 μg ml^{-1} while observable toxicity can be seen at 100 μg ml^{-1}. In all types of cells, nanoparticles are preferentially either adhered to the cell membrane or internalized into the cells. For the cell lines Fe_3O_4 nanoparticles could be used as a drug carrier, where the least toxicity of Fe_3O_4 nanoparticles was observed. Whereas in the case of other cell lines where substantial toxicity was observed, we can use them for cancer therapy. This observation also reveals that either bipolar surfactant and/or Fe_3O_4 nanoparticles are biocompatible in the range of 0.1–10 μg ml^{-1} towards normal as well as glia and breast cancer cells. The plausible mechanisms of cytotoxicity/cellular uptake of Fe_3O_4 nanoparticles in general are demonstrated. These results also further imply that more study into the internalization of Fe_3O_4 is both warranted and essential with regard to the toxicity of nanomaterials [41, 42]. This is indispensable to reveal its biocompatibility and biosafety for *in vivo* use.

Acknowledgment

This work was supported by grants from the National Science Council of Taiwan (NSC 97-2113-M-002-012-MY3).

References

[1] Ito A, Shinkai M, Honda H and Kobayashi T 2005 *J. Biosci. Bioeng.* **100** 1–11
[2] Pankhurst Q A, Connolly J, Jones S K and Dobson J 2003 *J. Phys. D: Appl. Phys.* **36** 167–81
[3] Vasir J K and Labhasetwar V 2005 *Technol. Cancer Res. Treat.* **4** 363–74
[4] Scherer F *et al* 2002 *Gen. Ther.* **9** 102–9
[5] Jordan A *et al* 1999 *J. Magn. Magn. Mater.* **194** 185–96
[6] Moroz P, Jones S K and Gray B N 2002 *Int. J. Hyperth.* **18** 267–84
[7] Kircher M F, Allport J R, Zhao M, Josephson L, Lichtman A H and Weissleder R 2002 *Radiology* **225** 453
[8] Lewin M *et al* 2000 *Nat. Biotechnol.* **18** 410–4
[9] Pisanic T R II, Blackwell J D, Shubayev V I, Finones R R and Sungho J 2007 *Biomaterials* **28** 2572–81
[10] Sun J *et al* 2007 *J. Biomed. Mater. Res.* A **80A** 333–41
[11] Gupta A K and Wells S 2004 *IEEE Trans. Nanobiosci.* **3** 66–73
[12] Tsoli M, Kuhn H, Brandau W, Esche H and Schmid G 2005 *Small* **1** 841–4
[13] Goodman C M, McCusker C D, Yilmaz T and Rotello V M 2004 *Bioconjug. Chem.* **15** 897–900
[14] Gupta A K and Gupta M 2005 *Biomaterials* **26** 1565–73
[15] Yin H, Too H P and Chow G M 2005 *Biomaterials* **26** 5818–26
[16] Predoi D, Barsan M, Andronescu E, Vatasescu-Balcan R A and Costache M 2007 *J. Optoelect. Adv. Mater.* **9** 3609–13

[17] Horie M *et al* 2009 *Chem. Res. Toxicol.* **22** 543–53
[18] Huang M, Khor E and Lim L Y 2004 *Pharm. Res.* **21** 344–53
[19] West J L and Halas N J 2003 *Annu. Rev. Biomed. Eng.* **5** 285–92
[20] Jain K K 2005 *Technol. Cancer Res. Treat.* **4** 407–16
[21] Wu X *et al* 2003 *Nat. Biotechnol.* **21** 41–6
[22] Chan W C W, Maxwell D J, Gao X, Bailey R E, Han M and Nie S 2002 *Curr. Opin. Biotechnol.* **13** 40–6
[23] Alivisatos A P 2004 *Nat. Biotechnol.* **22** 47–52
[24] Sokolov K *et al* 2003 *Technol. Cancer Res. Treat.* **2** 491–504
[25] Hirsch L R *et al* 2003 *Proc. Natl Acad. Sci. USA* **100** 13549–54
[26] Ankamwar B, Chaudhary M and Sastry M 2005 *Syn. React. Inorg. Metal Org. Nano-Metal Chem.* **35** 19–26
[27] Shiv Shankar S, Rai A, Ankamwar B, Singh A, Ahmad A and Sastry M 2004 *Nat. Mater.* **3** 482–8
[28] Berry C C, Wells S, Charles S and Curtis A S G 2003 *Biomaterials* **24** 4551–7
[29] Zhang Y, Kohler N and Zhang M 2002 *Biomaterials* **23** 1553–61
[30] Huang J H, Parab H J, Liu R S, Lai T C, Hsiao M, Chen C H, Sheu H S, Chen J M, Tsai D P and Hwu Y K 2008 *J. Phys. Chem.* C **112** 15684–90
[31] Greenhalgh K G and Turos E 2009 *Nanomed. Nanotech. Biol. Med.* **5** 46–54
[32] McCarron P A, Marouf W M, Quinn D J, Fay F, Burden R E, Olwill S A and Scott C J 2008 *Bioconjug. Chem.* **19** 1561–9
[33] Tomitaka A, Hirukawa A, Yamada T, Morishita S and Takemura Y 2009 *J. Magn. Magn. Mater.* **321** 1482–4
[34] Sun S *et al* 2004 *J. Am. Chem. Soc.* **126** 273–9
[35] Wang L *et al* 2005 *J. Phys. Chem.* B **109** 21593–601
[36] Stoeva S I, Huo F, Lee J S and Mirkin C A 2005 *J. Am. Chem. Soc.* **127** 15362–3
[37] Vogel A I *et al* 1989 *Textbook of Practical Organic Chemistry* (Harlow: Addison Wesley Longman)
[38] Silverstein R M, Bassler G C and Morrill T C 1991 *Spectrometric Identification of Organic Compounds* (New York: Wiley)
[39] Mitra S, Gaur U, Ghosh P C and Maitra A N 2001 *J. Control. Release* **74** 317–23
[40] Auffan M, Achouak W, Rose J, Roncato M A, Chaneac C, Waite D T, Masion A, Woicik J C, Wiesner M R and Bottero J Y 2008 *Environ. Sci. Technol.* **42** 6730–5
[41] Nel A, Xia T, Madler L and Li N 2006 *Science* **311** 622–7
[42] Service R F 2005 *Science* **310** 1609